Available online at www.sciencedirect.com
SCIENCE DIRECT®
Journal of Nuclear Materials 352 (2006) 357–364
journal of nuclear materials
www.elsevier.com/locate/jnucmat

Thoria, a quasi-inert matrix for actinides dispositions

D. Barrier, A.A. Bukaemskiy *, G. Modolo

Institut für Sicherheitsforschung und Reaktortechnik, Forschungszentrum Jülich GmbH, D-52425 Jülich, Germany

Abstract

Thoria is a promising matrix for the immobilisation of plutonium in either a burning or a conditioning strategy. The aim of this work is twofold: to study the impact of the addition of plutonium, simulated with cerium, on the physico-mechanical properties of thoria and to investigate the possibility of synthesising ceramics employing simple fabrication routes. $Th_{1-x}Ce_xO_2$ powders with ceria concentrations from 0 to 75% were synthesised by the co-precipitation method. The properties of the powders, such as thermal and crystallisation behaviour, were determined as a function of ceria content and calcination temperature. $(Th,Ce)O_2$ pellets containing up to 20% ceria were compacted from non-ground 675 K calcined powder using a double repressing method. The pellets have densities of up to 0.98 TD and a homogeneous surface with well-distributed pores. The main mechanical properties, such as microhardness and fracture toughness, were also investigated as a function of ceria content.

PACS: 61.66.B; 81.20.E; 62.20.M; 68.37.E,H,L,N

1. Introduction

The partitioning and transmutation strategy of plutonium and the minor actinides has been proposed for the reduction of the long-term radiotoxicity of nuclear waste. Transmutation requires the development of dedicated fuels. Alternatively, after partitioning, the actinides can be conditioned into stable dedicated solid matrices (partitioning & conditioning strategy) [1]. Thorium oxide is a very attractive matrix from a waste minimisation point of view. In fact, by using thoria as a support for burning plutonium in LWRs, the actinide production is very low and thus the consumption rates of Pu are very high [2–5]. Moreover, thoria is also a chemically inert matrix and very resistant to leaching, so that it can be used as an inert matrix for final disposal [6,7].

ThO_2–PuO_2 system was already well investigated and the fabrication of thorium oxide pellets, spheres, or coated particles is well known [1]. However, some data about the impact of the addition of plutonium on the thermal and crystallisation behaviour of the material are missing. Moreover, thorium matrix may be used for further immobilisation of trivalent actinides particularly in the case of a conditioning strategy. In this case easy fabrication processes and homogeneous final material being required [1]. Because, the co-precipitation method

* Corresponding author. Tel.: +49 2461 614574; fax: +49 2461 612450.
E-mail address: a.bukaemskiy@fz-juelich.de (A.A. Bukaemskiy).

0022-3115/$ - see front matter © 2006 Elsevier B.V. All rights reserved.
doi:10.1016/j.jnucmat.2006.03.001

is among the simplest techniques for rapid synthesis of large amounts of material and chemically homogeneous for powder synthesis it appears as an interesting method. However, the main disadvantage of this method is the formation of interparticle bonds during drying that cause particle aggregation/agglomeration [8]. Thus a grinding–milling step is usually required to reduce the agglomerate size and so improve the sinterability of powders.

The aim of the present work is twofold:

(1) to study the impact of the addition of tetravalent actinides, simulated in this work by cerium, on the properties of the matrix;
(2) to investigate the possibility of synthesising thoria-based ceramics for plutonium burning and storage by using co-precipitation methods without milling step.

In the present study, several oxide powders composed of thoria and ceria ($Th_{1-x}Ce_xO_2$), with a ceria ratio (x) varying from 0 to 75 mol%, have been synthesised by co-precipitation. In fact, cerium shows properties similar to plutonium. These elements are isostructural and have nearly identical cation radii. Besides, the lattice constants for PuO_2 (0.5395 nm) and for CeO_2 (0.5411 nm) are close together [9,10]. The thermal behaviour of the powders and the peculiarities of material crystallisation have been investigated. Pellets containing ceria from 0 to 20% were fabricated, utilising powders prepared by co-precipitation, without milling, using a pressing by repressing method, and their microstructure and mechanical properties were also investigated as a function of ceria concentration.

2. Experimental procedure

2.1. Synthesis of $Th_{1-x}Ce_xO_2$ powders and pellets

$Th_{1-x}Ce_xO_2$ powders with ceria contents of 0, 5, 10, 15, 20, 25, 50, and 75 mol% were synthesised by the co-precipitation method. $Th(NO_3)_4 \cdot 5H_2O$ (Merck, p.a.) and $Ce(NO_3)_3 \cdot 6H_2O$ (Alfa Aesar, 99.9%) were used as initial materials. The required quantity of the salt was dissolved in deionised water at room temperature, reaching a concentration of approximately 10^{-2} mol/L. On stirring, ammonia gas was used for co-precipitation. To ensure a slow and homogeneous precipitation, NH_3 was added to the surface of the solution until the reaction was complete. Precipitates were then separated, washed by deionised water, and finally dried at 385 K for 24 h. After drying, the powders were calcined in air at 675 K for 5 h. Approximately 1g of the non-ground powders was pressed by cold uniaxial pressing into cylindrical pellets of 10 mm diameter. The powders were compacted by using a double repressing method at 890 MPa. The pellets were then sintered at 1875 K for 5 h in air atmosphere in an electric resistance furnace (Linn HT 1800). The employed heating rate from room temperature to 1875 K was 5 K min^{-1}.

2.2. Characterisation

The thermal behaviour of the powders was investigated by thermogravimetry (TG) and differential scanning calorimetry (DSC) in air with a heating rate of 10 K min^{-1} using a Netzsch STA 449C Jupiter apparatus. The crystal structure of the powders was investigated by X-ray diffraction (XRD) using a Stoe transmission diffractometer system, STADI, (Cu, $\lambda = 1.540598$ Å). The lattice parameters were determined using the Nelson–Riley method [11].

Sintered pellets were carefully polished with diamond paste (1 μm) for further investigations of the microstructure. For SEM investigations, the samples were thermally etched in air at 1775 K for 1 h and then their morphology was analysed. The densities of the samples were measured by hydrostatic weighing in water. The theoretical densities were calculated from the XRD results [12].

The microhardness H_V (GPa) of sintered samples was measured by a diamond Vickers indenter (Anton Paar MHT 10) applying a load (F) of 4 N. The microhardness was calculated by the following expression [13]:

$$H_V = 1852F/d^2, \quad (1)$$

where F (N) represents the load and d (μm) the average length of the diagonals of the Vickers indents. The fracture toughness K_{IC} (MPa $m^{0.5}$) was estimated by the indentation crack length method using the Antis expression [13]:

$$K_{IC} = 0.032 \cdot H_V \cdot (d/2)^{0.5} \cdot (E/H_V)^{0.5} \cdot (2c/d)^{-1.5}, \quad (2)$$

where c (μm) represents the average length of cracks and E (GPa) the Young modulus.

The Young modulus was estimated as a function of the ceria content, C_{Ce} (%), and the relative porosity of the ceramics η (%) as

$$E = E^{\circ}_{Ce}(1 - 2.9\eta), \quad (3)$$

where E°_{Ce} is the Young modulus of a dense ceramic with a concentration of cerium C_{Ce}. Eq. (3) and the factor 2.9 were taken from [14]. The value E°_{Ce} was estimated for each ceria content by a linear dependence between $E^{\circ}_{ThO_2} = 249$ GPa [15] and $E^{\circ}_{CeO_2} = 165$ GPa [16].

3. Results and discussion

3.1. TG-DSC analysis

After synthesis and drying at 385 K, the thermal behaviour of powders containing up to 75% ceria was investigated by TG-DSC in air atmosphere. All powders show similar behaviour, as represented in Fig. 1 for the case of 50% ceria. As shown in Fig. 1(a), the thoria-ceria powder presents a two-step mass loss (8.15%) from 300 to 950 K. In the temperature range from 300 to 650 K, the mass loss (5.20%) is accompanied by a heat consumption corresponding to the elimination of adsorbed and hydrated water and impurities. From 665 (T_I) to 950 K (T_F) a second endothermic effect with a minimum at 770 K (T_M) and an enthalpy $\Delta H = -65.5$ J g^{-1} is observed on the DSC curve. This effect is accompanied by a second significant mass loss (2.95%). Heating at temperatures higher than 1350 K (T_S) is necessary to stabilise the mass.

$CeO_2 \cdot nH_2O$ (Alfa Aesar, Reacton 99.9) was also investigated by thermal analysis (Fig. 1(b)). The mass of the sample first steeply decreases from 300 to 500 K and is accompanied by an endothermic effect also corresponding to the elimination of adsorbed water and impurities. By increasing the temperature to 725 K, the DSC curve shows a sharp exothermic effect at 561 K followed by an endothermic effect whose minimum is located at 610 K. These effects are accompanied by another decrease of mass (6.7%). The sharp exothermic peak still remains if the sample is heated in inert atmosphere (N_2) and certainly corresponds to the elimination of impurities and not to the oxidation of Ce(III) [17]. Heating at temperatures higher than 1050 K stabilises the mass.

The effect of the addition of ceria is clearly observed on the characteristic parameters (T_I, T_M, T_F, T_S, and ΔH) of the system (Fig. 2). As defined in the case of 50% ceria (cf. Fig. 1), T_I, T_M, and T_F correspond to the temperature of the beginning, the minimum, and the end of the second endothermic peak, respectively. T_S is the temperature of the stabilisation of mass and ΔH the enthalpy of the second endothermic peak. If T_F remains constant at around 955 K, T_I and T_M first slightly decrease up to a ceria concentration of 20% and then decrease tending to the values of pure ceria. Simultaneously, the intensity of the endothermic peak ΔH also decreases from −13.1 to −79.9 J g^{-1}

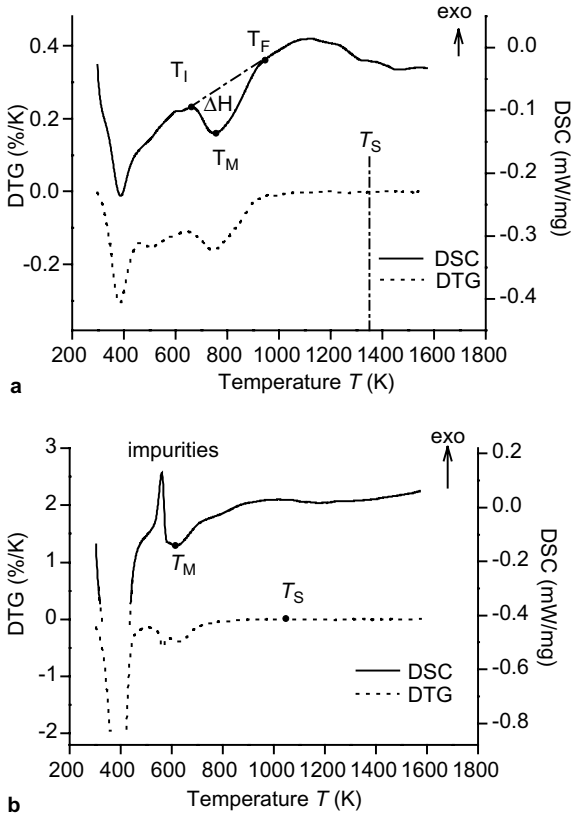

Fig. 1. DTG and DSC curves of $Th_{0.50}Ce_{0.50}O_2$ (a) and pure CeO_2 (b) powder in air atmosphere.

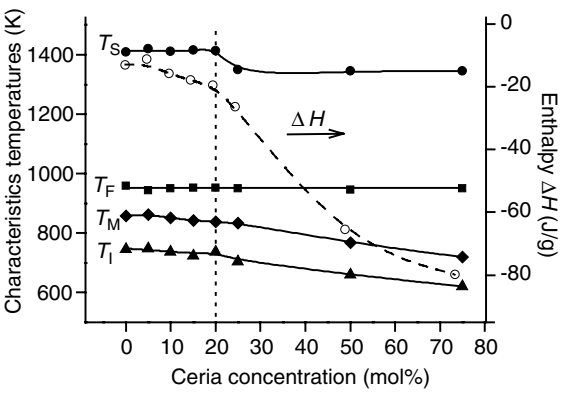

Fig. 2. Influence of ceria concentration on the characteristic temperatures T_I, T_M, T_F and T_S and the enthalpy ΔH.

with ceria addition, following the same behaviour as the temperatures T_I and T_M. Moreover, T_S remains constant at 1410 ± 10 K for ceria concentrations of up to 20% and then decreases to 1340 ± 10 K for higher ceria contents.

Thus, the physical properties of the $Th_{1-x}Ce_xO_2$ system can be divided into two regions as a function of ceria concentration: from 0 to 20% and from 20 to 100%. In the first region, the investigated properties (T_I, T_M, T_F, T_S, and ΔH) remain constant and are mainly determined by the properties of the thoria matrix. In the second region, the properties tend to the properties of ceria.

3.2. XRD analysis

According to the TG-DSC results, pure thoria and ceria, and the powders containing 10, 25 and 50% ceria were calcined in the DSC furnace at 475, 575, T_I, T_M, T_F, 1375 and 1875 K before XRD analysis.

Pure thoria and ceria crystallise after drying in a face-centred cubic (fcc) fluorite-type structure. Their lattice parameter a (Å) continuously decreases with increasing calcination temperature (Fig. 3). Their lattice parameters were determined as a function of mass loss (Δm), as defined in Eq. (4):

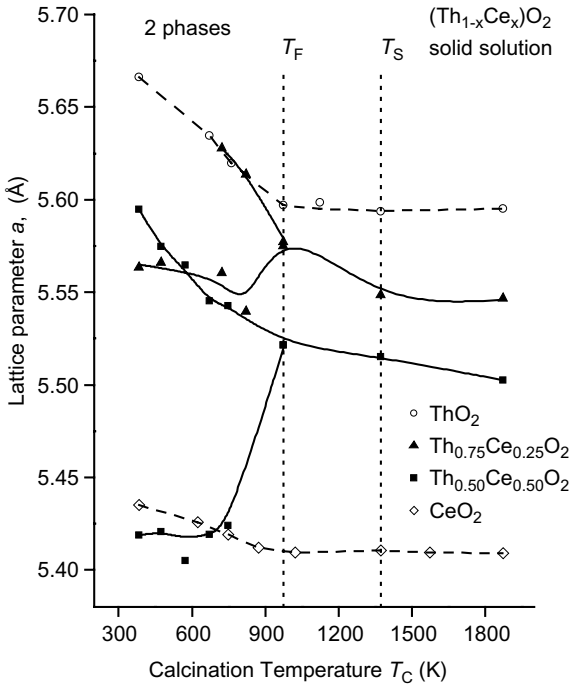

Fig. 3. The lattice parameter of ThO_2, CeO_2, $Th_{0.75}Ce_{0.25}O_2$ and $Th_{0.50}Ce_{0.50}O_2$ as a function of the calcination temperature.

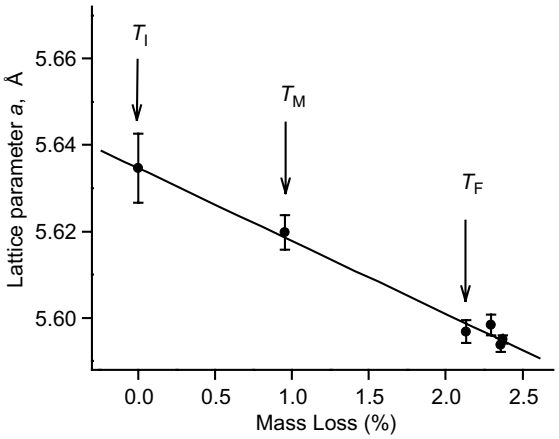

Fig. 4. The lattice parameter as a function of mass loss for ThO_2.

$$\Delta m = [m(T_I) - m(T)]/m(T_I). \quad (4)$$

As represented in Fig. 4 in the case of pure ThO_2, the lattice parameter has a linear dependence on the mass loss. The linear correlation confirms that the lattice parameter is determined by the presence of OH groups in the material [18].

Thus, the endothermic peaks observed on the DSC curves at $T_M = 857$ and 614 K for thoria and ceria are representative of the elimination of the OH groups present in the lattice.

According to XRD, the $ThCeO_2$ system containing 10% of cerium crystallises after drying in a $(Th,Ce)O_2$ solid solution, fcc fluorite-type structure. By increasing the temperature, the lattice parameter of this system also decreases. However, contrary to pure ThO_2, no linear dependence between the lattice parameter and the mass loss in the temperature range from T_I to 1825 K can be established. The second endothermic peak observed on the DSC curves can be described not only by the elimination of OH groups of the $(Th,Ce)O_2$ system.

After drying and at calcination temperatures lower than T_F, the XRD peaks of the powders containing 25, 50 and 75% ceria can be decomposed into 2 Gaussians revealing the presence of two separate phases, fcc fluorite type, in the powder. Thus, in the case of 25%, after drying, the system is mainly composed of pure thoria and of a $(Th,Ce)O_2$ solid solution with a deficiency of thorium. $ThCeO_2$ powders with ceria concentration of 50 and 75% mainly consist of pure CeO_2 and of a $(Th,Ce)O_2$ solid solution with a deficiency of cerium. All these systems (ThO_2, CeO_2 and $(Th,Ce)O_2$) crystallise in a fcc, fluorite-type structure.

The lattice parameter was thus determined for each concentration as a function of the calcination temperature (Fig. 3).

By increasing the calcination temperature up to T_I, the lattice parameter of the different systems decreases. At the calcination temperature T_F, the XRD lines are sufficiently sharp, so that they cannot be clearly described by two separated Gaussians. In this case, the average value of the XRD lines was used for the determination of lattice parameter a. At T_F, the a value tends to the value of the lattice parameter of a $(Th_{1-x}Ce_x)O_2$ solid solution. Further heating up to T_S (1375 K) results in a complete solid solution formation. The lattice parameter then remains fairly constant with temperature.

These results can be extended to powder with low ceria concentrations. In fact, ThO_2 has a low crystallinity degree after calcination at low temperature and the determination of this additional phase by the XRD method is therefore difficult. Moreover, in the case of 10% ceria, the clear stoichiometry of the observed XRD phase could not be established. Considering these facts, powders containing up to 25% ceria were certainly composed of $(Th, Ce)O_2$ solution and a segregation of ThO_2, that could only be clearly detected as a separate phase in the case of 25% ceria.

It is well known form the literature [9,10,19–22], ThO_2–CeO_2 system and ThO_2–PuO_2 system crystallises at high temperature in a fcc solid solution, fluorite type and that their lattice parameters follow the Vegard's law. For control, the powders were calcined at 1875 K. All powders crystallise in a fcc solid solution, fluorite type, and their lattice parameters follow the Vegard's law:

$$a = -0.1849x + 5.5945. \quad (5)$$

Our data correlates very well with the data obtained in the literature [9,10,19,20].

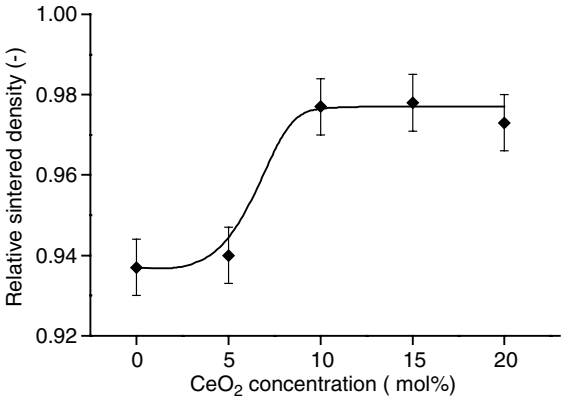

Fig. 5. Dependence of relative sintered densities of pellets on ceria content.

Table 1
Evolution of the lattice parameter (calculated and experimentally determined) of $(Th, Ce)O_2$ and $(Pu, Th)O_2$ powders calcined at 1875 K, with the cerium/plutonium fraction x in mol%; relative standard deviation, σ

	$(Th, Ce)O_2$					$(Pu, Th)O_2$		
x (mol%)	a_{Model} (nm)	a_{exp} (nm)	σ (%)	a [19] (nm)	σ (%)	a_{Model} (nm)	a [21] (nm)	σ (%)
0.0	0.5601	0.5595	0.11	0.5599	0.03	0.5601	0.5598	0.05
5.0	0.5592	0.5585	0.12	–	–	–	–	–
10.0	0.5582	0.5576	0.12	0.5577	0.10	–	–	–
15.0	0.5573	0.5567	0.12	–	–	0.5570	0.5568	0.03
20.0	0.5564	0.5557	0.12	0.5559	0.09	–	–	–
25.0	0.5555	0.5547	0.15	–	–	–	–	–
26.0	–	–	–	–	–	0.5547	0.5546	0.01
30.0	0.5546	–	–	0.5542	0.06	–	–	–
36.9	–	–	–	–	–	0.5524	0.5526	0.03
40.0	0.5527	–	–	0.5519	0.15	–	–	–
46.7	–	–	–	–	–	0.5504	0.5502	0.04
50.0	0.5509	0.5505	0.08	0.5504	0.09	–	–	–
60.0	0.5490	–	–	0.5486	0.08	–	–	–
63.5	–	–	–	–	–	0.5469	0.5469	0.00
70.0	0.5472	–	–	0.5464	0.14	–	–	–
75.0	0.5463	0.5458	0.08	–	–	–	–	–
80.0	0.5453	–	–	0.5445	0.15	–	–	–
82.5	–	–	–	–	–	0.5430	0.5428	0.03
90.0	0.5435	–	–	0.5427	0.15	–	–	–
100.0	0.5417	0.5409	0.14	0.5414	0.05	0.5393	0.5396	0.05

However, if the lattice parameter of $(Th_{1-x}Pu_x)O_2$ obtained by XRD follows the Vegard's law, it has been recently demonstrated by Heisbourg et al. [23] that the next neighbour and the next near neighbour distances given by XAFS investigation, do not follow this law. This type of behaviour may be extended to our system and to other tetravalent actinides, since the difference between the radius of Th^{4+} and the immobilised actinide is large.

$(Th, Ce)O_2$, extendly $(Th, Pu)O_2$, crystallise in a stable fluorite type structure, where metal atoms have a coordination number (CN) of 8 and oxygen atoms have a CN of 4. According to the Ingel and Lewis model [24], in the case of a fluorite structure, the lattice parameter a can be defined as following:

$$a = 4(r^- + r^+)/\sqrt{3}, \tag{6}$$

where r^- and r^+ are the ionic radius of the anionic and cationic species, respectively. The ionic radius r^+ should be considered as an average of all ionic radii, expressed as

$$r^+ = \sum_i xiRi, \tag{7}$$

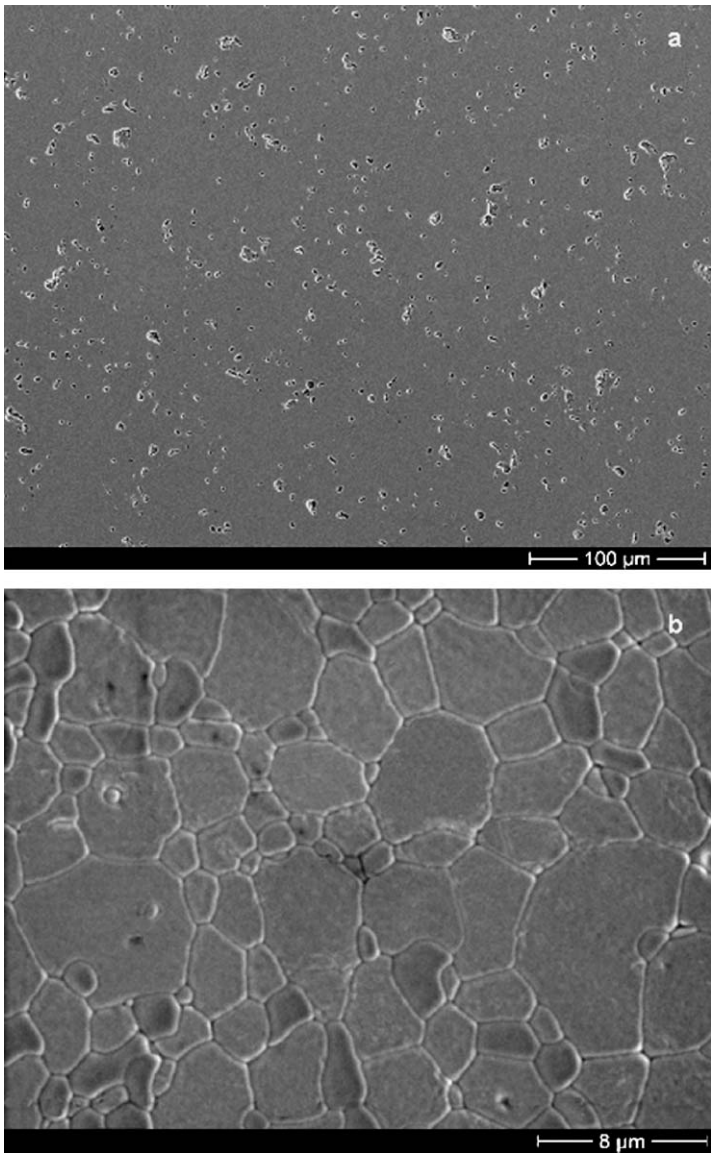

Fig. 6. SEM photographs of $(Th_{0.90}Ce_{0.10})O_2$ pellets sintered at 1875 K for 5 h.

where x_i is the fraction and R_i the ionic radius of the species i at fixed CN.

The Th^{4+}, Ce^{4+} and Pu^{4+} have a ionic radius of 0.105, 0.097 and 0.096 nm, respectively [25]. The lattice parameter of $(Th, Ce)O_2$ and $(Th, Pu)O_2$ system were so theoretically determined as a function of the Ce or Pu concentration (Table 1) and the data were compared with the experimental data obtained for powder after calcination at 1875 K (from this work and from the work of [19] and [21]). The calculated data well correlates to the experimental data and the deviation are 0.1% and 0.03% in the case of Ce and Pu, respectively. The Ingel and Lewis model can so be used to describe both systems.

3.3. Sintering behaviour and physico-mechanical properties of pellets

$(Th, Ce)O_2$ pellets were fabricated with ceria concentrations from 0 to 20%. After calcination at 675 K for 5 h, the powders were directly pressed by repressing, applying 3 times a pressure of 890 MPa. The relative density of the pellets was determined as a function of ceria addition (Fig. 5). The density of the pellets reaches a value of 0.94 TD for pure thoria and 5% ceria and then steeply increases up to 0.98 TD for concentrations of 10 to 20% ceria. This significant increase may be correlated with a decrease of the agglomerate strength of the powders by addition of ceria, which allow an easier crashing and reorganisation of agglomerates during the compaction and so enhance the sinterability. Moreover, the addition of cerium enhances the sinterability of thorium [26]. Similar behaviour were observed in the case of plutonium [22,27]. Recently, within the framework of the European Thorium Cycle Project, ThO_2 and $(Th, Pu)O_2$ pellets were prepared by the sol–gel route, for an irradiation experiments in the High-Flux Reactor in Petten. The pellets containing 11% plutonium have a higher density than pure ThO_2 [2].

After sintering, the pellets were polished, thermally etched at 1775 K for 30 min and their surfaces investigated by SEM. For all ceria contents, the pores are well distributed in the matrix (Fig. 6(a)) and mainly located at the grain boundaries. The pores have an irregular shape and can be very large, reaching a size of up to 10 μm. This effect can be explained by the non-homogeneity of the initial packing. Moreover, the surface is composed of grains (Fig. 6(b)) with well-formed grain boundaries. However, they have an irregular curvature.

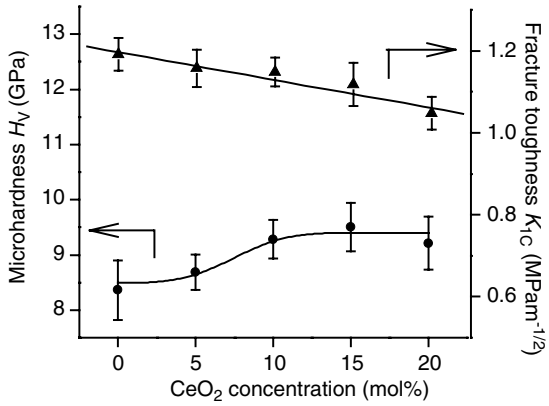

Fig. 7. Dependence of microhardness (H_V) and fracture toughness (K_{IC}) on ceria concentration.

The grains have a maximum size of 8.0 μm with an average grain size of 2.4 μm.

The dependence of the microhardness H_V and fracture toughness (K_{IC}) of the pellets on the ceria content was also investigated. The microhardness of the pellets increases with ceria addition from 8.6 to 10.3 GPa, correlating with the evolution of pellet density (Fig. 7). As described in [28], ThO_2 pellets with a density of 95% have a Vickers hardness of 7 GPa. According to the work of Maschio et al. [29], a ceramic of pure CeO_2 with a density of 0.94 TD has a microhardness of 3.9 GPa. Since both systems have a similar crystal structure, it is supposed that the addition of ceria to the ThO_2 matrix will decrease the mechanical properties of the matrix [29]. Moreover, Basak et al. [30] prepared $Pu_{0.04}Th_{0.96}O_2$ pellets of 92% density and measured a Vickers hardness of 3.4 GPa at 400 K. An extrapolation of the data to room temperature gives a value of 4 GPa. Thus, the addition of Pu is also supposed to decrease the mechanical properties. However, in our case, the addition of ceria leads to an increase of sintered pellet density (Fig. 6) and the mechanical properties of the material increase with increasing density [31]. Thus, for ceria contents from 5 to 25 wt%, the high increase in density of the pellets has a good effect on microhardness.

The fracture toughness of the pellets linearly decreases with ceria from 1.20 to 1.05 MPa $m^{-1/2}$. The data obtained for pure thoria correlates well with the literature [32].

4. Conclusion

The thermal and crystallisation behaviour of the ThO_2–CeO_2 system was studied in detail for

different ceria concentrations. After drying, ThO_2 and CeO_2 crystallise in a fcc fluorite-type structure. During heating, they exhibit endothermic behaviour due to the elimination of OH groups from the lattice.

In addition, $Th_{1-x}Ce_xO_2$ systems present an endothermic character, corresponding also to the elimination of OH-groups. However, after drying the $Th_{1-x}Ce_xO_2$ powders mainly consists of two fcc phases:

- a $(Th,Ce)O_2$ solid solution and pure ThO_2 for ceria contents less than 25%;
- a $(Th,Ce)O_2$ solid solution and pure CeO_2 for ceria contents higher than 50%.

Heating these $Th_{1-x}Ce_xO_2$ powders at temperatures between 960 and 1410 K leads to the formation of a $Th_{1-x}Ce_xO_2$ solid solution, which also crystallises in a fcc fluorite-type structure. At high calcination temperature, the system follows Vegard's law.

$(Th,Ce)O_2$ pellets were fabricated from non-ground powders by using a repressing process and reached densities of up to 0.98 TD. For all ceria contents, the pellets show a homogeneous microstructure with well-distributed pores that have an irregular shape and can be large, reaching a size up to 10 μm. The microhardness and fracture toughness of the pellets were investigated and are very sensitive to the density variation of the system.

Acknowledgement

This work was supported by the European Union (EUROPART, Contract No F16W-CT-2003-508854). The authors would like to express their thanks to W. Reichert for performing the XRD measurements and Dr M. M. Titov for performing SEM measurements.

References

[1] R.J.M. Konings, Advanced fuel cycles for accelerator-driven systems: fuel fabrication and reprocessing, EU report 19928, 2001.
[2] R.P.C. Schram, J.C. Kuijper, D. Sommer, J. Somers, P. Phlippen, T. Bodewig, A. Worral, C. Struzik, Ph. Raison, in: Proc. of the International Workshop on P&T and ADS Development 2003, Mol, Belgium, 6–8 October 2003.
[3] H. Akie, T. Muromura, H. Takano, S. Matsura, Nucl. Technol. 107 (1994) 182.
[4] C. Lombardi, A. Mazzola, E. Padovani, M.E. Ricotti, J. Nucl. Mater. 274 (1999) 181.
[5] C. Lombardi, L. Luzzi, E. Padovani, F. Vettraino, Prog. Nucl. Energ. 38 (2001) 395.
[6] S. Hubert, K. Barthelet, B. Fourest, G. Lagarde, N. Dacheux, N. Baglan, J. Nucl. Mater. 297 (2001) 206.
[7] C.F. Baes, R.E. Mesmer, The Hydrolysis of Cations, Wiley-Interscience, New York, 1976, p. 129.
[8] G. Hare'l, B.G. Ravi, R. Chaim, Mater. Lett. 39 (1999) 63.
[9] J.G. Pepin, G.J. McCarthy, J. Am. Ceram. Soc. 64 (9) (1981) 511.
[10] S. Peterson, C.E. Curtis, Thorium Ceramics Data Manual ORNL-4503 i (1970) 41.
[11] C. Winston, Analytical chemistry by open learning: X-ray methods, Wiley, New York, 1985, p. 132.
[12] H. Yahiro, K. Egushi, H. Arai, Solid State Ionics 36 (1989) 71.
[13] D. Munz, T. Fett, Ceramics: Mechanical Properties, Failure Behaviour, Materials Selection, Springer, Berlin Heidelberg, 1999, p. 31.
[14] R.W. Rice, Porosity of Ceramics, Marcel Dekker, Inc., Berlin Heidelberg, 1998, p. 276.
[15] J. Belle, R.M. Berman, Thorium Dioxide: Properties and Nuclear Applications, Government Printing Office, Washington, DC, 1984.
[16] Molycorp, Inc., Cerium, a guide to its role in chemical technology, Moutain Pass, CA, USA, 1992, p. 12.
[17] G.M. Ingo, G. Righini, L. Scoppio, Appl. Surf. Sci. 55 (4) (1992) 257.
[18] A.A. Bukaemskiy, D. Barrier, G. Modolo, J. Eur. Ceram. Soc. 26 (2006) 1507.
[19] A.K. Tyagi, B.R. Ambekar, M.D. Mathews, J. Alloys Compd. 337 (2002) 277.
[20] Gmelin Handbuch, Thorium, System-Nr 44, Ergänzungsband Teil C2 (1976) 78.
[21] R.N.R. Mulford, F.H. Ellinger, J. Phys. Chem. 62 (11) (1958) 1466.
[22] M.D. Freshley, H.M. Mattys, Irradiation of $(Th,Pu)O_2$, thorium fuel cycle, US Atomic Energy Commission, Oak Ridge, Tenn., February 1968, p. 463.
[23] G. Heisbourg, J. Purans, Ph. Moisy, S. Hubert, Local structure of $Th_{1-x}M_xO_2$ solid solutions with M = U, Pu, in: Proc. of Actinides 2005, Manchester, Great Britain, 4–7 July 2005.
[24] R.P. Ingel, D. Lewis III, J. Am. Ceram. Soc. 6 (4) (1986) 225.
[25] J.A. Dean, Lange's Handbook of Chemistry, 14th Ed., McGraw-Hill, New York, 1992, p. 4.13.
[26] R.B. Pinheiro, F.S. Lameiras, M. Peehs, V. Maly, Thorium utilisation in LWRs, Final Report (1979–1988), KFA Jül-Spez 488, 1988, p. 152.
[27] T.R.G. Kutty, P.V. Hegde, J. Banerjee, K.B. Khan, A.K. Sengupta, G.C. Jain, S. Majumdar, H.S. Kamath, J. Nucl. Mater. 312 (2003) 224.
[28] S. Peterson, C.E. Curtis, Thorium Ceramics Data Manual ORNL-4503 i (1970) 20.
[29] S. Maschio, O. Sbaizero, S. Meriani, J. Eur. Ceram. Soc. 9 (1992) 127.
[30] U. Basak, A.K. Sengupta, C. Ganguly, J. Mater. Sci. Lett. 8 (4) (1989) 449.
[31] R.W. Rice, Porosity of Ceramics, Marcel Dekker, Inc., 1998, 276.
[32] J. Belle, R.M. Berman, Thorium dioxide: Properties and Nuclear applications, Government Printing Office, Washington, DC, 1984.